Water Research X 2 (2019) 100023

Contents lists available at ScienceDirect

Water Research X

journal homepage: https://www.journals.elsevier.com/water-research-x

Two-dimensional ammonium distribution in sediment pore waters using a new colorimetric diffusive equilibration in thin-film technique

Edouard Metzger [a, *], Anthony Barbe [a], Florian Cesbron [a, b], Aubin Thibault de Chanvalon [a, c], Thierry Jauffrais [a, 1], Didier Jézéquel [d], Aurélia Mouret [a]

[a] LPG-BIAF, UMR 6112, Université d'Angers, 2 Bd Lavoisier, 49045, Angers Cedex, France
[b] University of West Florida, Center for Environmental Diagnostics and Bioremediation, 11000 University Parkway, Pensacola, FL, 32514, USA
[c] School of Marine Science and Policy, University of Delaware, Lewes, DE, 19958, USA
[d] Institut de Physique du Globe de Paris, Université Sorbonne Paris Cité, Univ. Paris Diderot, UMR 7154 CNRS, 75005, Paris, France

ARTICLE INFO

Article history:
Received 7 August 2018
Received in revised form
13 December 2018
Accepted 15 December 2018
Available online 20 December 2018

Keywords:
Biogeochemistry
High-resolution
Porewater
DET
Densitometry

ABSTRACT

This study presents a new gel based technique to describe the pore water ammonium distribution through the sediment-water interface in two dimensions at a millimeter scale. The technique is an adaptation of the classical colorimetric method based on the Berthelot's reaction. After the thin film of the gel probe was equilibrated by diffusion either in standard solutions or in pore waters, a colorimetric reagent gel was set on the gel probe, allowing development of the characteristic green color. A flatbed scanner and subsequent densitometry image analysis allowed to determine the concentration distribution of ammonium. The gel probe was tested in the laboratory for two media, deionized water and seawater, within the range 0–3000 μM in NH_4^+. Detection limit is about 20 μM and accuracy about ±25 μM. The field validation was realized in a tidal mudflat of the French Atlantic coast by comparison with conventional pore water extraction and colorimetric analysis. The large range of concentrations and its applicability in continental and marine sediments suggest a wide range of applications of the technique for a reasonable cost.

1. Introduction

In benthic coastal ecosystems, ammonium is the most abundant nitrogenous form and is used preferentially in autotrophic reactions rather than nitrite and nitrate (Horrigan and McCarthy, 1982; Ivančič and Degobbis, 1984). Then, ammonium is recycled by micro and microbenthic fauna during remineralization of organic matter (Regnault, 1987), including shorebirds (Jauffrais et al., 2015) and tends to accumulate in the anoxic layer of sediments (Herbert, 1999). Therefore, its availability to microalgae and macrophytes depends on its upward flux to the photic layer of the sediment (Welker et al., 2002). Ammonium is involved in several redox reactions such as reduction of manganese oxide, anammox or nitrification influencing other biogeochemical cycles (Luther et al., 1997; Anschutz et al., 2000; Dalsgaard and Thamdrup, 2002; Deflandre et al., 2002). Physical transport such as advection, tidal pumping and bioirrigation, may generate important spatial heterogeneity within the sediment (Santos et al., 2012). As a consequence, the rapid transfer of superficial water into the sediment may affect ammonium distribution at the scale of burrows enhancing for instance nitrification (Welsh and Castadelli, 2004). At a millimeter scale, ammonium heterogeneity has never been documented in sediment pore waters, whereas, it is documented for other nutrients such as phosphorus (Pagès et al., 2011; Cesbron et al., 2014; Ding et al., 2016) and nitrite and nitrate (Metzger et al., 2016). See Santner et al. (2015) for an extensive review of pore water imaging techniques. Since ammonium is a nitrogen species playing a major role in primary and secondary early diagenetic reactions, achieving its 2D distribution at high spatial resolution combined with other imaging techniques will help understanding nutrients and metal remobilization dynamics in coastal habitats. Furthermore, it will improve our knowledge, at fine scale, of such habitats often exposed to anthropogenic pressure, especially in a context of climate change and oxygen depleted zones spreading (Diaz and Rosenberg, 2009).

* Corresponding author.
E-mail address: edouard.metzger@univ-angers.fr (E. Metzger).
[1] Current address: Ifremer, RBE/LEAD, 101 Promenade Roger Laroque, 98897, Nouméa, New Caledonia.

https://doi.org/10.1016/j.wroa.2018.100023

Several analytical techniques exist to measure ammonium concentration in aquatic environments. Among them, a well-known colorimetric method is the Berthelot reaction (Berthelot, 1859). This method is based on the reaction between ammonia, a phenol and sodium hypochlorite in an alkaline solution that creates a blue complex (wavelength of maximum absorbance of 690 nm). Color intensity corresponds to the sum of ammonium and ammonia concentrations in the sample. Through time this method was improved and adapted to different natural environments (Riley, 1953; Harwood and Kühn, 1970; Patton and Crouch, 1977; Ivančič and Degobbis, 1984). Another photometric technique is based on fluorescence properties of ammonium in a solution; this method allows detection of very low concentration (about 100 nM). However, the kinetics of the reaction is very slow (about 3 h) and the reagent is highly photosensitive (Holmes et al., 1999). To avoid fluorometric measurement limitations, ammonium can also be measured by Flow Injection Analysis (Kérouel and Aminot, 1997; Holmes et al., 1999). Detection by selective electrode (Garside et al., 1978) and by cathodic stripping voltammetry (Harbin and van den Berg, 1993) also exist but demand a large volume of sample (several ml).

All these techniques need an initial separation of pore waters from sediments by squeezing or centrifugation of core slices. The pore water characterization is a difficult task at high spatial resolution (*i.e.* below few mm) with these sampling methods as they are limited by the pore water volumes collected during extraction. Furthermore, this resolution is insufficient to describe numerous biogeochemical processes occurring at millimeter scale that are typical of highly productive coastal environments. In addition, current methods show numerous disadvantages associated with the extraction procedure such as cellular lysis of living organisms during centrifugation that might give inaccurate measurements (Mudroch and MacKnight, 1994). The development of *in situ* microelectrodes during the 80s allowed to measure at high resolution the ammonium concentration (de Beer and Sweerts, 1989), but its use to study lateral variability remains time consuming, reducing its spatial relevance. In addition, the technique is sensitive to alkaline ions and is not applicable in marine waters. Planar optodes were also developed to characterize the ammonium turnover around roots (Strömberg, 2008), but their applicability *in situ* remain limited due to their cost and complexity. For all these reasons, we developed an inexpensive and easy to use, 2D-DET colorimetric technique for *in situ* ammonium analysis as an alternative to current analytical techniques.

This technique is based on the diffusion between pore waters and a hydrogel layer that contains 95–98% water according to its composition (polyacrylamide or agarose, respectively). The main challenge with 2D-DET colorimetric techniques is to find the best compromise between reaction kinetics, reagents concentration and diffusion in order to limit lateral diffusion causing relaxation of potential microenvironments (Cesbron et al., 2014; Jézéquel et al., 2007; Metzger et al., 2016). This method has already been developed successfully for iron, phosphates, alkalinity, and more recently for nitrite and nitrate (see references above) and is now adapted for the first time to ammonium. This new method was then validated by comparison with current analytical methods for pore waters analysis of sediment cores.

2. Material and methods

2.1. Colorimetric principle

The first step of the reaction consists to raise the solution pH up to 11 with sodium hydroxide to convert ammonium into ammonia that reacts with sodium hypochlorite to form monochloramine. Then, monochloramine reacts with a phenolic compound to form a blue dye (2,2'diisopropyl-5,5'dimethyl-indophenol blue) that absorbs light at 690 nm. A phenol commonly used is thymol; it can be replaced by sodium salicylate, a less toxic (Searle, 1984) but less sensitive compound (Krom, 1980). Sodium nitroprusside is added to catalyze this reaction. In marine environments, the high concentrations of calcium and magnesium (about 10 and 53 mM, respectively (Millero et al., 2008)) interfere in the reaction (Riley, 1953). These alkali-earth elements precipitate with carbonate when the solution pH is raised with sodium hydroxide. To prevent precipitation, chelating agents such as CDTA (cyclohexyl-trans-1,2-diaminetetraacetid acid) (Roskam and De Langen, 1964) or sodium citrate are used to complex magnesium and calcium. However, sodium citrate is photosensitive (Bower and Holm-Hansen, 1980), we thus replaced it by etidronic acid, another chelating agent used in the Merck (©) ammonium kit.

2.2. Gel probe preparation and deployment

The preparation of the 2D-DET probe and its colorimetric analysis is adapted from Jézéquel et al. (2007). The probe is a polycarbonate plate (250 mm high, 150 mm width and 2 mm thick) with a central depression (180 mm long × 92 mm wide × 1 mm thick). This depression holds an agarose hydrogel that is covered by a PVDF porous membrane (0.2 µm, Durapore ®), which is affixed with a PVC tape. The gel layer is prepared with 1.5 g of pure agarose (Sigma-Aldrich, CAS: 9012-36-6) dissolved in 100 mL of MilliQ water at 80 °C. To have a homogeneous gel thickness, the heated agarose solution is quickly poured vertically between 2 polycarbonate plates separated by a U-frame of 1 mm thickness. The whole setting is then chilled in a fridge for few minutes to accelerate the gelation. The probe is rinsed and stored with/in MilliQ water until use. Unlike other 2D-DET gel probes made for iron, alkalinity, phosphorus, or nitrate and nitrite analysis, the use of polyacrylamide is prohibited because preliminary tests have shown that polyacrylamide reacts with the ammonium reagent probably because of its amide groups. Polyacrylamide gels are usually preferred to agarose despite their toxicity and additional preparation steps due to their softness and strength that make it handier to use than agarose gels. However, the 1 mm thickness used for the probe preparations is sufficient to have a robust and easy to use agarose gel despite its large dimensions.

To avoid oxygen contamination during probes deployment within the sediment, the probes are deoxygenated by nitrogen bubbling in MilliQ water overnight before deployment. The probes are then inserted in the sediment at two thirds of their total length and kept until chemical equilibrium with pore waters.

2.3. Calibration and reagent gel preparation

Ammonium standard solutions were prepared by dissolution of NO_3NH_4 salt (Fluka CAS: 6484-52-2) in a solution of adequate ionic strength. Seven standard solutions from 0 µM to 500 µM, or 3000 µM according to the test, were placed in contact to a 1 mm-thick agarose gel for 1 h (see details in Cesbron et al., 2014) and further processed as a probe gel.

The color development of the *in situ* gel is achieved using two agarose gels equilibrated in reagent solutions for at least 30 min. Indeed, unlike previous methods that use one single reagent gel (Jézéquel et al., 2007; Pagès et al., 2011; Bennett et al., 2015; Metzger et al., 2016), two reagent gels are required for the reaction because reagents are not stable when mixed all at once. The first colorimetric reagent solution contains 0.65 M sodium hydroxide (Sigma Aldrich CAS: 1310-73-2), 0.012 M sodium hypochlorite (Sigma Aldrich CAS: 7681-52-9), and 0.12 M etidronic acid (Sigma Aldrich CAS: 2809-21-4) in deionized water (Millipore, Milli-Q

system). The second coloring reagent solution contains 0.027 M sodium nitroprusside (Fluka CAS: 13755-38-9) and 0.12 M thymol (Sigma Aldrich CAS: 89-83-8) in deionized water. The latter reagent has to be prepared in two steps because thymol needs a non-aqueous solvent to be incorporated to the final reagent solution, here methanol (5% thymol in methanol). Reagent gels are exposed to 50 mL of their respective reagent solution in a plastic bag and gently mixed for at least 30 min for equilibration. It is recommended to keep the bag on a stirring table to facilitate homogenization.

2.4. Gel assemblage and colorimetric reaction

After equilibration, reagent gels are removed from their respective bags and quickly drained before being laid down onto white plates. After having wiped the drops of residual reactive solution, the "probe gel" (i.e. the one deployed in the field) is laid onto the first "reagent gel". The second "reagent gel" is immediately placed on the assembled gels. The three-layer gel assemblage is then covered by a clean cellulose acetate film to avoid evaporation. Gradually the typical color of the indophenol blue develops; associated with the yellow nitroprusside in alkaline medium, it gives a green final color. Finally, after 20 min of reaction at room temperature (~20 °C), the three-layer gel assemblage is scanned to acquire the 2D ammonium distribution in the sediment pore waters.

2.5. 2D imagery methods

To obtain the ammonium distribution, a simple commercial flatbed scanner (Canon Canoscan LiDE 152 600F) was used. From scanned images, intensity of coloration of the 2D probe was processed with ImageJ® software (Schneider et al., 2012). Images were at first stripped from their edges (5 mm) in order to avoid any edge effect and then decomposed into primary color intensities (red, green and blue at about 140 nm wavelength resolution), each being converted to a gray-scale image. The red color intensity was found to give the most sensitive response, since the dye formed is blue. As this channel can saturate with high ammonium concentration, the less sensitive green channel can also be used (See Results and Discussion section). A region of interest (ROI) is selected for each zone of the "standard gel" corresponding to a circle of about 15 mm in diameter (i.e. 30,000 pixels with the selected resolution); this circle was the zone of equilibration of the gel with the standard solution.

2.6. Optimization tests

The principle of the 2D-DET methods developed to date (Jézéquel et al., 2007; Robertson et al., 2008; Pagès et al., 2011; Cesbron et al., 2014; Bennett et al., 2015; Metzger et al., 2016), is to adapt preexisting colorimetric reaction for solutions to the hydrogel 2D samples, by superimposing one or two reagent gels over a sample gel that was previously equilibrated in the sediment. The colorimetric method that was considered as a reference method to be adapted for the 2D determination was the colorimetric test from Merck (Spectroquant©), which is derived from Harwood and Kühn (1970). The main difference between both protocols resides in the use of etidronic acid in our method to prevent interferences from alkali-earth elements by chelation. Briefly, in the Harwood and Kühn (1970) method a volume of sample reacts with a series of reagents that are concentrated to ensure excess for all reagents. In our case, the protocol combining gel layers induced a dilution of a factor three (case of two reagent gels) leading to possible changes in sensitivity and importance of interferences. Therefore, optimization of reagent concentrations is necessary. This testing was performed in two steps: a first phase in spectrophotometric cuvettes in order to limit volume of chemicals and a second phase in gels by narrowing ranges found in the first stage. The transposition from solutions to gels is not automatic since cross diffusion processes may affect locally kinetics and order of reactions in the case of a series of reactions to reach the colored indophenol dye. These processes may induce precipitate formations that also affect analytical performance. In the following sub-sections, we explore the concentration of the catalyst in the kinetics of the development of the indophenol dye, secondly the importance of the chelating agent when working in seawater and then the amount of thymol in both a solution and a gel assemblage.

2.7. Field validation

This technique was applied in the intertidal mudflat of Bourgneuf Bay. The Bay is located south of the Loire estuary on the French Atlantic coast (Fig. 1) and is characterized by a presence of wild oyster reefs (Echappé et al., 2018) and oyster and mussel farming areas.

The field validation consisted to deploy a 2D-DET probe near an observation site (47°00'56.9"N 2°02'27.6"W) where sediment geochemistry was documented on a monthly basis. The survey consisted of sampling three cores of 10 cm in diameter at each vertex of an equilateral triangle of 10 m (Fig. 1, right panel). Sampling was carried out in June 2016 at low tide, salinity was 33 and the temperature of the sediment was 18 °C. The 2D-DET probe was deployed for three hours within the sediment for equilibration between the gel and pore waters. Then the probe was carefully collected with its surrounding sediment that represents a slab of 3 cm of thickness using a "jaw device" (Thibault de Chanvalon et al., 2015) and transported to the laboratory to reach an equilibration time of 5 h in total. The jaw device was then opened and the 2D-DET probe processed immediately. The sediment cores were kept at *in situ* temperature until processing the next day.

2.8. Core processing and pore water analyses

The cores were sliced under nitrogen atmosphere every 2 mm to a depth of 2 cm, then every 5 mm to a depth of 5 cm, and finally every centimeter to 11 cm depth. Sediment slices were immediately centrifuged at 3500 rpm for 15 min and the supernatant was filtered using a 0.2 µm filter (RC25, Sartorius©). One aliquot was frozen for colorimetric analysis (ammonium, nitrite and nitrate), a second one was acidified and diluted for total Fe, Mn, P, Si and S analysis, and a third aliquot was used for immediate analysis of alkalinity. Ammonium was analyzed using a phenol-hypochlorite method (Harwood and Kühn, 1970), with etidronic acid as chelating agent to prevent magnesium and calcium precipitation. Alkalinity was measured using the colorimetric bromophenol blue/formic acid method (Sarazin et al., 1999). All spectrophotometric analyses were performed using a Genesys 20 from Thermo-Fischer. Fe, Mn, P, Si and S measurements were performed after a 50-fold dilution with a 1% ultrapure nitric acid with an ICP-OES ICAP 6300 Thermo-Fischer. Analyzed elemental sulfur was interpreted as sulfate since sulfide is volatile and was removed from the sample solution under acidic conditions (pore water samples were acidified at pH below 1 for storage before ICP-OES analysis).

3. Results and discussion

3.1. Optimization tests

3.1.1. Influence of nitroprusside content in the reagent

A series of standard curves were realized using different sodium

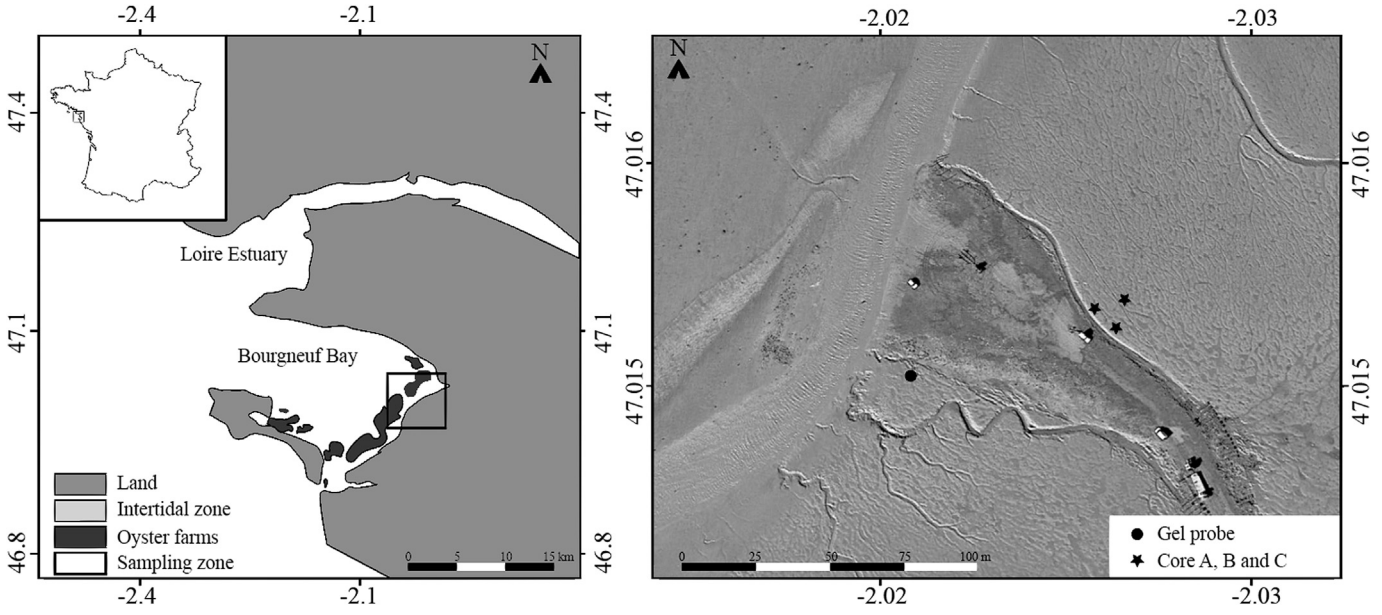

Fig. 1. Location of the Bourgneuf Bay (left panel). Location of sampling sites (right panel). The 2D-DET deployment site is marked by a circle. The cores sampling sites are marked by stars.

nitroprusside concentrations within a range from 0.025 to 0.056 M. Nitroprusside being a catalyst for the formation of the monochloramine-thymol intermediate compound (N-chloro-2,isopropyl-5,methyl-quinone-monoimine), the absorbance was measured at different times (between 10 and 20 min), and at different concentrations of ammonium (between 15 and 1000 μM). Results did not show any variability within the range of nitroprusside concentrations. This test did not show any effect of time either. It suggests that a concentration of 0.025 M of sodium nitroprusside is concentrated enough to observe the complete formation of the indophenol blue in 10 min within a range of ammonium concentrations from 30 to 1000 μM. At 15 μM of ammonium results were comparable to blanks. For the final protocol a concentration of 0.025 M of sodium nitroprusside was retained for the reagent.

When moving to the gel, the time retained for analysis after contact between gel probe and reagent gel was 20 min in order to allow diffusion and colorimetric reaction between gels.

3.1.2. *Importance of etidronic acid*

Two calibration curves for ammonium were carried out in spectrophotometric cuvettes (Fig. 2). The two calibrations differed by the use or not of etidronic acid as a chelating agent to complex alkali-earth elements that are susceptible to precipitate when sodium hydroxide is added rising pH over 13. Without etidronic acid, one can observe the rise of the intercept by a factor three, a slight

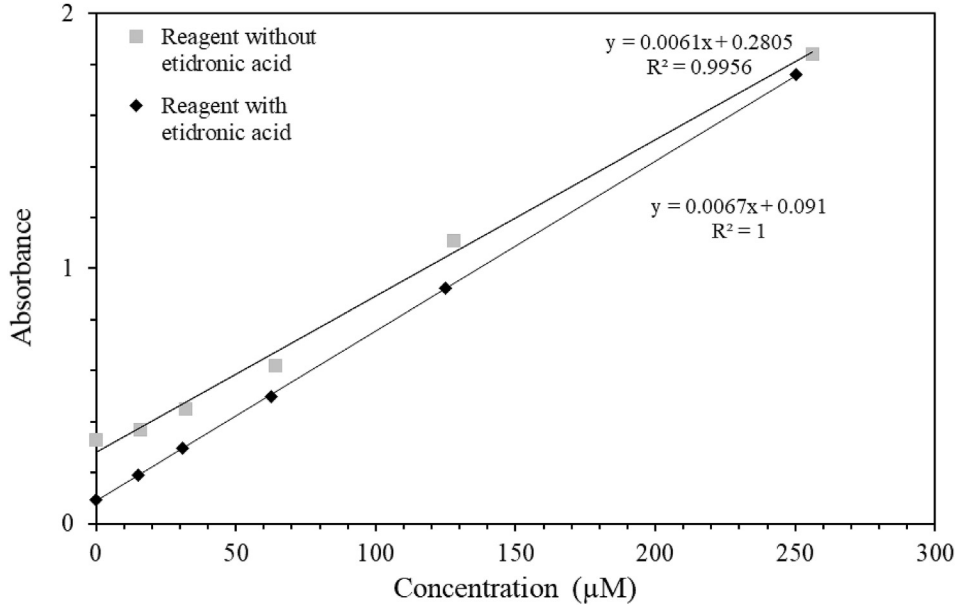

Fig. 2. Calibration curves of ammonium in artificial seawater. These calibrations were performed in spectrophotometric cuvettes. Grey squares represent a calibration without etidronic acid, black diamonds are for a calibration with etidronic acid. Wavelength: 690 nm.

diminution of the slope (about 10%).

Furthermore, the presence of precipitates in current analytical method for ammonium is less dramatic as particles may settle in the cuvette below the path of the beam light. However, in the case of a gel thin-films, the precipitates cannot be removed. As the color of the surface is measured (*i.e.* reflectance), the presence of precipitates can have dramatic consequences at the pixel scale.

3.1.3. Influence of thymol concentration

Six calibration curves were performed in cuvettes to assess the optimal thymol concentration (0.012 M–0.018 M – 0.03 M–0.06 M – 0.09 M–0.12 M, Fig. 3). All curves follow a linear pattern with similar slopes (0.0039 ± 0.002) and R^2 above 0.992. These results suggest that even at the lowest concentration, there is enough thymol to react with the monochloramin within the range of 0–500 μM ammonium.

A simplified version of the previous test was performed on gel layers: only two concentrations of thymol were tested, 0.06 and 0.12 M (Fig. 4). With a thymol concentration of 0.06 M (grey squares), the calibration curve shows a slope of −0.106 and $R^2 = 0.94$ up to 260 μM of ammonium; whereas using 0.12 M thymol (dark diamonds), the slope is −0.076 and $R^2 = 0.991$. Despite a rather lower slope, the experiment using a higher amount of thymol shows a better linearity and a lower dispersion. The linear correlation seems not to fit well with data indicating a probable saturation of the reagent with the lower concentration of thymol. These results highlight the difficulty to transfer colorimetric techniques in cuvettes to gel layers. The hydrophobic property of thymol probably explains the necessity to increase the amount of thymol in the reagent for gel layer protocol. The high volatility of methanol, the solvent of thymol, may also affect the colorimetric reaction: the high surface/volume ratio enhances the evaporation of methanol and consequently the precipitation of thymol that will obviously affect the coloration reading. This can also explain the apparent saturation effect in the experiment using 0.06 M of thymol (better fit of a polynomial curve for the dark dots). Therefore, 0.12M of thymol was the concentration retained for the field-based tests.

3.2. Calibration curves

Standardization of images can be done using the red and the green channel of images after splitting color channels. The protocol presented here shows a linear relation between ammonium concentration of pore waters and gray intensity for the red channel within the range 0–500 μM ($R^2 = 0.9964$, Fig. 5A) and within 0–3000 μM for the green channel ($R^2 = 0.9943$, Fig. 5A and B). The blue channel gray intensity shows almost no relation with ammonium concentration and will not be considered thereafter. The red channel is the most sensitive channel, as it covers the wavelengths corresponding to the absorption peak of the green colored indophenol compound formed by the reaction. This result enhances the range of use of the method. Indeed, users can calibrate their 2D-DET probes with ammonium concentrations ranged between 0 and 500 μM using the red channel with a precision of about 25 μM (using a linear regression model; 95% percent of confidence) and a detection limit of 17 μM ammonium (corresponding to three times the blank of the standard curve). The same channel can be used in a broader range by applying a polynomial relationship. Fig. 5A indicates that up to 2000 μM, a quadratic polynomial is acceptable ($r^2 = 0.9998$; precision of about 100 μM within the range 1000–2000 μM). However, if the 2D-DET probe shows results beyond that range, users can switch to the green channel that shows a linear relationship with ammonium concentration up to 3000 μM. Despite a drop of precision (about 250 μM), the linearity of the relation allows the user to transform over ranged reflectance data into concentration.

3.3. Reproducibility of standardization

Several standard calibration curves were performed with the optimized protocol to assess the reproducibility of the method. The slopes and intercepts of the different standard calibration curves showed variations of 12% and 17%, respectively ($n = 6$) for a series of experiments performed in a 3-months period. The variation at the intercept is attributed to the dilution of the nitroprusside, for which

A

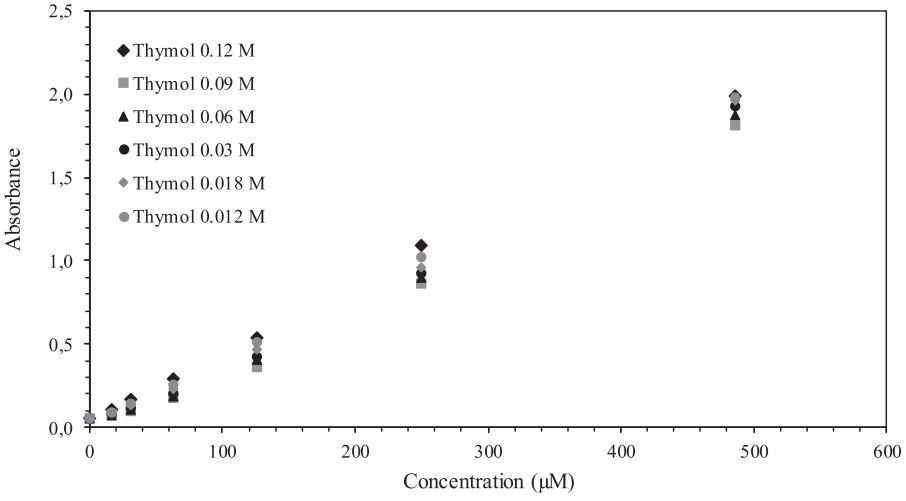

B

[Thymol]	0.12M	0.09M	0.06M	0.03M	0.018M	0.012M
Slope	0.004	0.0037	0.0038	0.0039	0.004	0.004
R^2	0.9992	0.9929	0.9949	0.9958	0.9978	0.9995

Fig. 3. A) Comparison of six standard calibration curves with different concentrations of thymol. B). Slope and R^2 values for each standard calibration curve as a function of thymol concentration.

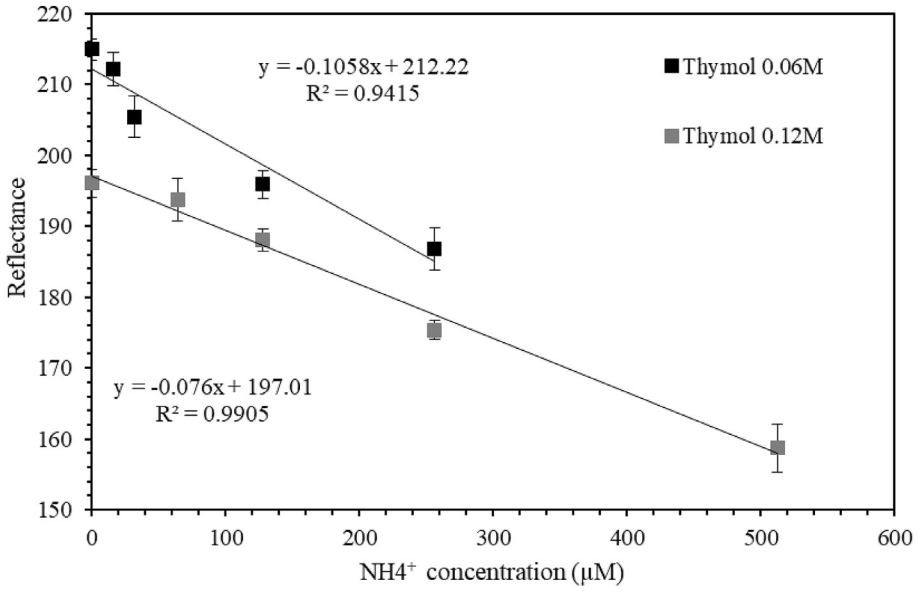

Fig. 4. Comparison of two standard calibration curves with different concentrations of thymol. Grey squares correspond to a thymol concentration of 0.06 M against 0.12 M for dark diamonds. This test was performed on agarose gel (1 mm thickness).

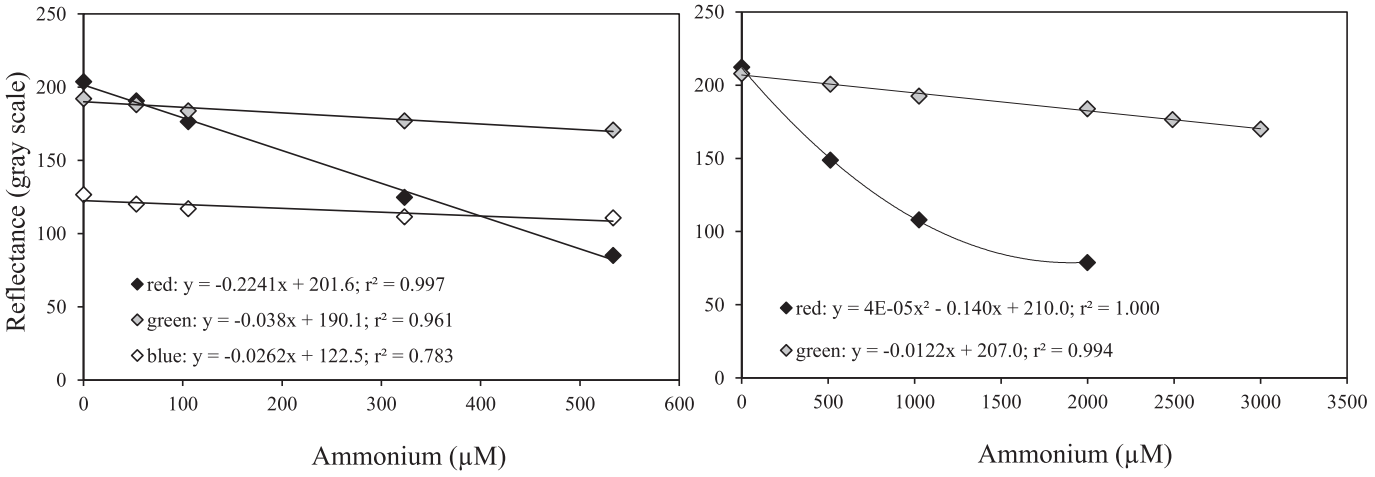

Fig. 5. Standard calibration curves for two 2D-DET gels and 2 ammonium ranges. Black diamonds: red channel. Grey diamonds: green channel. White diamonds: blue channel. Standard deviation for each measurement is within the size of the symbol. Fig. 5A: concentration range of the standard calibration curve between 0 and 550 µM. Fig. 5B: concentration range of the standard calibration curve between 0 and 3000 µM.

broad reflectance spectrum covers the red channel used for ammonium quantification. The slope variation may be due to the sum of variability in dilution of each reagent that occurs in the chain of reactions until the blue dye is formed. Another set of experiments realized one year after, showed sensitivity 60% higher probably due to a different stock of reagents. To bypass such difficulties, it is recommended to prepare a fresh batch in a sufficient amount of reagents that can be used for standard and probe gels for the same session of analysis and to limit time between standardization and probe analysis because of the volatility of different reagents such as hypochlorite or methanol.

3.4. Kinetics vs. lateral diffusion

Calibration curves established from gel at equilibrium with standard solutions discussed in the previous section also served to establish the colorimetric reaction kinetics between the calibration gel and both reagent gels. After assemblage of the three gels, a scan was realized every 5 mn in order to measure the increase of the intensity of the green color. After 15 min, no significant change was observed in the gray intensity for the red channel (data not shown) meaning that 20 min is a reasonable time to get a full reaction between ammonium and colorimetric reagents. The sequence of scans also showed that lateral diffusion was also not observable indicating that the green dye has a diffusion coefficient sufficiently low compared to its reaction kinetics to impeach lateral diffusion to affect significantly ammonium distribution during processing. This feature was already observed for nitrite, iron and phosphorus (Cesbron et al., 2014; Metzger et al., 2016). However, it was also demonstrated that during deployment in the sediment, a loss of fidelity of pore water distribution within microenvironments was possible meaning that the researcher must be cautious while interpreting sharp gradients at high spatial resolution. We suggest that ~1 mm represents the highest resolution at which chemical gradients can be reliably interpreted (Harper et al., 1997; Metzger et al., 2016).

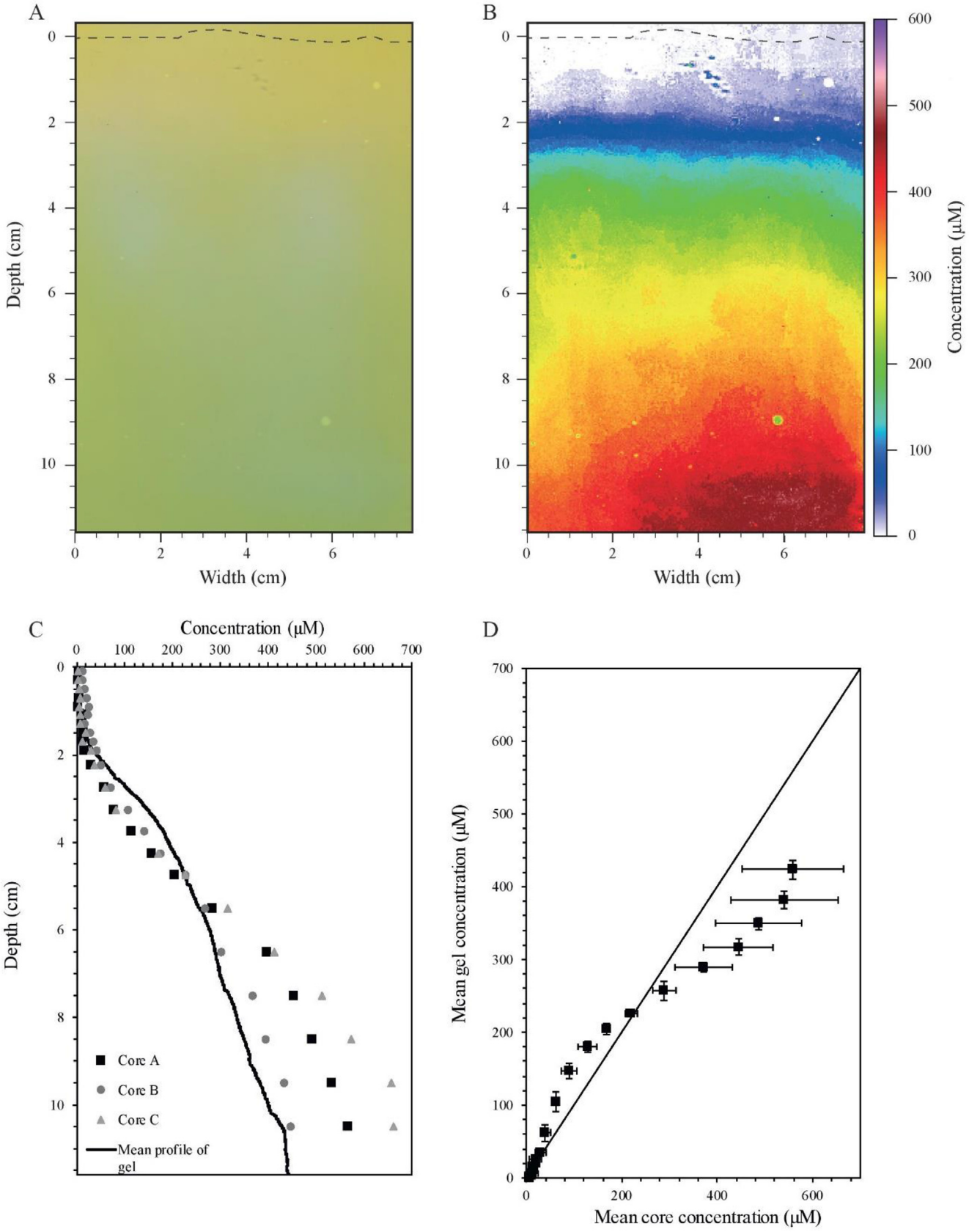

Fig. 6. A) 2D-DET scan. The dashed line represents the sediment/air interface. B) Standardized ammonium distribution in false color scale (µM). C) Comparison between results obtained from pore water extraction coupled to spectrophotometric analyses (squares, diamonds and circles) and a profile calculated using the average value of each pixel line of the 2D-DET scan. D) Relation between the average concentrations in ammonium (µM) measured in the three cores and the average concentrations in ammonium (µM) found in the gel using rectangles of similar sizes than core slices. (For interpretation of the references to color in this figure legend, the reader is referred to the Web version of this article.)

3.5. In situ validation of the method

In order to validate the method, the 2D-DET probe was deployed in Bourgneuf Bay and compared with pore water profiling using slicing-centrifugation-sampling and classical spectrophotometric analysis (Fig. 6). The image obtained after scanning has a green-yellowish color corresponding to the reagent gel that turns more or less green according to the concentration in ammonium.

The 2D distribution of ammonium after calibration of the scan shows ammonium concentrations below the limit of detection (17 μM) of the method in the overlying water and in the first two centimeters of sediment (Fig. 6B). Then, the ammonium content increases to reach maximum concentrations between 370 and 450 μM ammonium at the bottom of the image (12 cm depth). The vertical ammonium profile calculated using the 2D-DET probe (mean concentration of each line of pixels) shows a profile in the same order of magnitude than the ammonium profiles obtained using conventional sediment pore waters analysis (e.g., Gieskes et al., 1991; Metzger et al., 2007) of marine sediment cores sampled in Bourgneuf Bay (Fig. 6C). The differences in ammonium concentration in cores compared to the 2D-DET probe, and between cores can be explained by the heterogeneity of mudflat systems at a metric to decametric scale. This heterogeneity was recently demonstrated with microphytobenthic biomass in Bourgneuf Bay using satellite imagery (Echappé et al., 2018). Another explanation of a higher content in pore waters after extraction (i.e. cores), as mentioned in the introduction, is the lysis of cells from bacteria, algae or foraminifera that store ammonium for their physiological needs during centrifugation that may lead to an over estimation of ammonium (Mudroch and MacKnight, 1994). Nevertheless, the results from cores validate the 2D-DET gel probe technique. Differences between the four profiles are about 50% while standard deviation along a pixel line within the gel is about 10% suggesting lower heterogeneity at the decimetric scale for ammonium.

3.6. Early diagenetic context and ammonium behavior

To include into a biogeochemical context our ammonium results, we present complementary pore water data from the sediment cores. In the study site, oxygen penetration depth was 1.9 ± 0.3 mm (18 profiles were performed in darkness with Clark-type electrodes from Unisense, data not shown). Fig. 7 shows the results for dissolved Fe, Mn, P, Si, SO_4^{2-} and alkalinity. The left panel (dissolved Fe and Mn) clearly shows a remobilization zone for manganese at 1 cm depth while iron shows a remobilization zone at 3 cm depth. This is a common feature in coastal sediments and is coherent to the thermodynamic ladder of electron acceptors used during bacterial mineralization processes (Froelich et al., 1979; Bethke et al., 2011; Yücel, 2013). However, it can be noted that the pore water concentrations of manganese and iron reach high concentrations (about 650 μmol L^{-1} and 1200 μmol L^{-1} for manganese and iron, respectively). Such high concentrations suggest a high pool of reactive oxides in an environment rich in organic matter. This may explain the absence of ammonium in the top 2 cm, suggesting an efficient anoxic oxidation of ammonium in the upper sediment by Mn oxides (Luther et al., 1997) or by nitrate (Dalsgaard and Thamdrup, 2002). The dissolved Si profile (central panel of Fig. 7) shows a remobilization of silica that can be attributed to the dissolution of diatom frustules during early diagenesis (Tréguer and Rocha, 2013). One can observe the variations of silica gradients suggesting different zones of remobilization. A first remobilization zone is observed within the first centimeter of sediment that would represent the layer of fast recycling of silica where diatoms have their highest biomass. In the *La Coupelasse* intertidal mudflat, the microphytobenthic biomass is concentrated in the first 2 mm of sediment with a peak around 500 μm according to light exposure and tide (Méléder et al., 2005). A second remobilization zone below the iron remobilization one would correspond to a slower loop of nutrient recycling in the anoxic sediment. The fast recycling loop observed suggested for silica also contribute to keep pore water ammonium and phosphorus content in the first centimeter of sediment below quantification limit (<15 μM). The increase of alkalinity concomitant to the decrease of sulfate suggest the occurrence of sulfate reduction below the iron remobilization zone (Berner et al., 1970; Metzger et al., 2007). This may be confirmed by the uptake of iron in the lower part of the profile while manganese seems to be buffered by thermodynamic equilibrium of carbonate phases (Burdige, 1993, 2006; Mucci et al., 2000). This ongoing process below the sampled layer of sediment may be an additional source of ammonium explaining the high ammonium

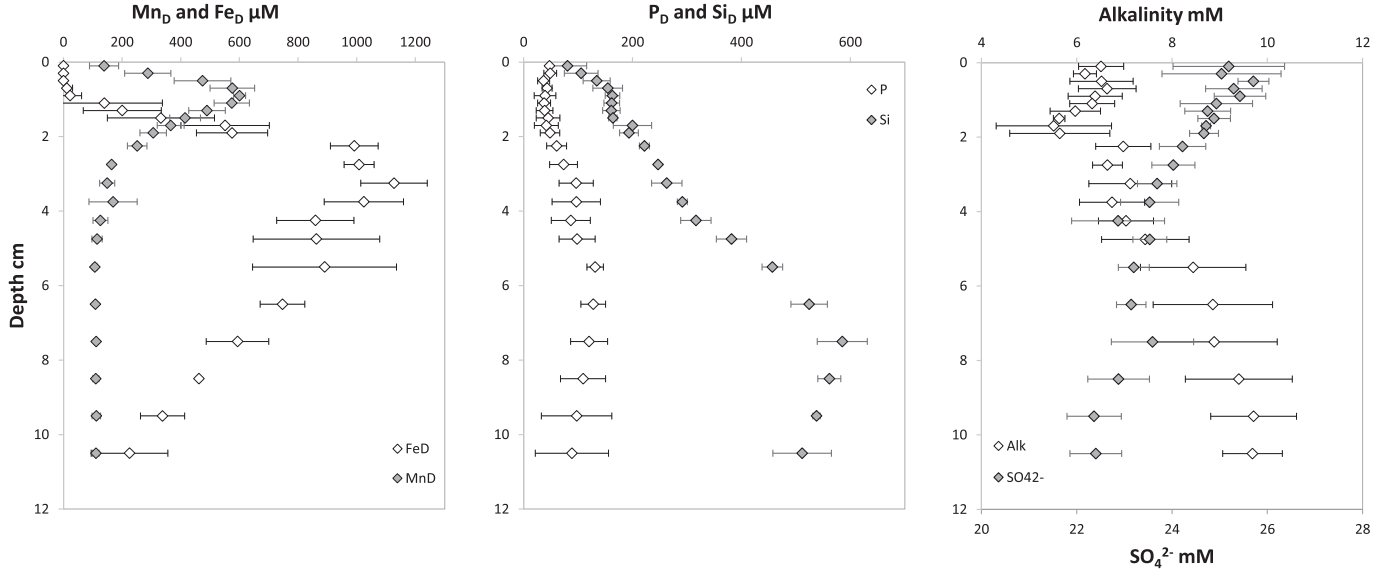

Fig. 7. Additional pore water data from the sediment cores sampled in Bourgneuf Bay. Total dissolved manganese and iron (left panel), total phosphorus and silica (central panel), and alkalinity and sulfate (right panel) profiles (n = 3).

concentrations observed at the bottom of the 2D-DET probe and sediment core profiles.

The variability between the 3 cores obtained from the calculation of the standard deviation decreases from Fe (rsd = 46 ± 55%) to P (rsd = 38 ± 16%) to Mn (rsd = 13 ± 10%) to Si (rsd = 8 ± 5%) to SO_4^{2-} (rsd = 2 ± 1%) to alkalinity (rsd = 1 ± 1%) which confirms the little lateral heterogeneity at a decametric scale with the exception of Fe and P. Paradoxically, decametric heterogeneity for dissolved iron is probably driven by lateral heterogeneity at the decimetric scale. Previous studies showed that after a bioirrigation event, the diffusive homogenization of iron is partially inhibited by the fast precipitation of iron oxides which maintain the heterogeneity (Thibault de Chanvalon et al., 2017). The fact that heterogeneity increases with depth for dissolved phosphorus suggests a buffering by adsorption on Fe oxides in the top 2 cm (Anschutz et al., 1998; Thibault de Chanvalon et al., 2016). Below, iron is remobilized and the heterogeneity of P increases precisely because of Fe heterogeneity.

4. Conclusions

The 2D-DET ammonium probe is a good alternative to the current ammonia pore water profiling (i.e., subsampling-centrifugation-analysis) that is sample- and time-consuming when performed at a millimeter vertical resolution. In addition, the technique allows 2D imaging for documenting lateral heterogeneities at a scale compatible to diatom biofilm patchiness, polychaetes burrowing or aquatic plants root development, either in marine and freshwater systems at the condition these features stand over deployment time (about 5 h The wide range of concentration (15–3000 μM) covered by the present protocol provides a well-adapted technique to describe chemical gradients in very rich systems such as dam sediments, sewage effluents. Finally, the present technique enriches the range of 2D DET methods to describe the fate of most of major chemical species related to early diagenetic processes (iron, phosphate, nitrite, nitrate, alkalinity, pH).

Declarations of interest

None.

Acknowledgements

This research was funded by the Region Pays de la Loire through the following projects: COSELMAR, FRESCO and OSUNA-RS2E. The French national program EC2CO-LEFE also financed this study through the project Manga-2D. This research is also supported with core data from the OSUNA project MUDSURV. Thanks to Eric Bénéteau and the interns Alan Nicol, Nicolas Dubosq, Joana Peschard, Romain Lévrard and Barnabé Cherville for their technical help. Thanks to the anonymous reviewers for their constructive comments that helped to greatly improve this manuscript.

References

Anschutz, P., Sundby, B., Lefrançois, L., Luther III, G.W., Mucci, A., 2000. Interactions between metal oxides and species of nitrogen and iodine in bioturbated marine sediments. Geochim. Cosmochim. Acta 64, 2751–2763. https://doi.org/10.1016/S0016-7037(00)00400-2.

Anschutz, P., Zhong, S., Sundby, B., Mucci, A., Gobeil, C., 1998. Burial efficiency of phosphorus and the geochemistry of iron in continental margin sediments. Limnol. Oceanogr. 43, 53–64.

Bennett, W.W., Welsh, D.T., Serriere, A., Panther, J.G., Teasdale, P.R., 2015. A colorimetric DET technique for the high-resolution measurement of two-dimensional alkalinity distributions in sediment porewaters. Chemosphere 119, 547–552. https://doi.org/10.1016/j.chemosphere.2014.07.042.

Berthelot, M.P.E., 1859. Répertoire de Chimie appliquée, vol. 1, pp. 284–293.

Berner, R.A., Scott, M.R., Thomlinson, C., 1970. Carbonate alkalinity in the pore waters of anoxic marine sediments. Limnol. Oceanogr. 15, 544–549. https://doi.org/10.4319/lo.1970.15.4.0544.

Bethke, C.M., Sanford, R.A., Kirk, M.F., Jin, Q., Flynn, T.M., 2011. The thermodynamic ladder in geomicrobiology. Am. J. Sci. 311, 183–210. https://doi.org/10.2475/03.2011.01.

Bower, C.E., Holm-Hansen, T., 1980. A salicylate–hypochlorite method for determining ammonia in seawater. Can. J. Fish. Aquat. Sci. 37, 794–798. https://doi.org/10.1139/f80-106.

Burdige, D.J., 2006. Geochemistry of Marine Sediments. Princeton Univ Pr.

Burdige, D.J., 1993. The biogeochemistry of manganese and iron reduction in marine sediments. Earth Sci. Rev. 35, 249–284. https://doi.org/10.1016/0012-8252(93)90040-E.

Cesbron, F., Metzger, E., Launeau, P., Deflandre, B., Delgard, M.-L., Thibault de Chanvalon, A., Geslin, E., Anschutz, P., Jézéquel, D., 2014. Simultaneous 2D imaging of dissolved iron and reactive phosphorus in sediment porewaters by thin-film and hyperspectral methods. Environ. Sci. Technol. 48, 2816–2826. https://doi.org/10.1021/es404724r.

Dalsgaard, T., Thamdrup, B., 2002. Factors controlling anaerobic ammonium oxidation with nitrite in marine sediments. Appl. Environ. Microbiol. 68, 3802–3808. https://doi.org/10.1128/AEM.68.8.3802-3808.2002.

de Beer, D., Sweerts, J.-P.R.A., 1989. Measurement of nitrate gradients with an ion-selective microelectrode. Anal. Chim. Acta 219, 351–356. https://doi.org/10.1016/S0003-2670(00)80369-4.

Deflandre, B., Mucci, A., Gagné, J.-P., Guignard, C., Sundby, B. jør, 2002. Early diagenetic processes in coastal marine sediments disturbed by a catastrophic sedimentation event. Geochim. Cosmochim. Acta 66, 2547–2558. https://doi.org/10.1016/S0016-7037(02)00861-X.

Diaz, R.J., Rosenberg, R., 2008. Spreading dead zones and consequences for marine ecosystems. Science 321, 926–929. https://doi.org/10.1126/science.1156401.

Ding, S., Wang, Y., Wang, D., Li, Y.Y., Gong, M., Zhang, C., 2016. In situ, high-resolution evidence for iron-coupled mobilization of phosphorus in sediments. Sci. Rep. 6. https://doi.org/10.1038/srep24341.

Echappé, C., Gernez, P., Méléder, V., Jesus, B., Cognie, B., Decottignies, P., Sabbe, K., Barillé, L., 2018. Satellite remote sensing reveals a positive impact of living oyster reefs on microalgal biofilm development. Biogeosciences 15, 905–918. https://doi.org/10.5194/bg-15-905-2018.

Froelich, P.N., Klinkhammer, G.P., Bender, M.L., Luedtke, N.A., Heath, G.R., Cullen, D., Dauphin, P., Hammond, D., Hartman, B., Maynard, V., 1979. Early oxidation of organic matter in pelagic sediments of the eastern equatorial Atlantic: suboxic diagenesis. Geochim. Cosmochim. Acta 43, 1075–1090. https://doi.org/10.1016/0016-7037(79)90095-4.

Garside, C., Hull, G., Murray, S., 1978. Determination of submicromolar concentrations of ammonia in natural waters by a standard addition method using a gas-sensing electrode1. Limnol. Oceanogr. 23, 1073–1076. https://doi.org/10.4319/lo.1978.23.5.1073.

Gieskes, J.M., Gamo, T., Brumsack, H., 1991. Ocean Drilling Program: Publications: Technical Note 15 (Technical Note No. 15).

Harbin, A.M., van den Berg, C.M.G., 1993. Determination of ammonia in seawater using catalytic cathodic stripping voltammetry. Anal. Chem. 65, 3411–3416. https://doi.org/10.1021/ac00071a013.

Harper, M.P., Davison, W., Tych, W., 1997. Temporal, spatial, and resolution constraints for in situ sampling devices using diffusional Equilibration: dialysis and DET. Environ. Sci. Technol. 31, 3110–3119. https://doi.org/10.1021/es9700515.

Harwood, J.E., Kühn, A.L., 1970. A colorimetric method for ammonia in natural waters. Water Res. 4, 805–811. https://doi.org/10.1016/0043-1354(70)90037-0.

Herbert, R.A., 1999. Nitrogen cycling in coastal marine ecosystems. FEMS Microbiol. Rev. 23, 563–590. https://doi.org/10.1111/j.1574-6976.1999.tb00414.x.

Holmes, R.M., Aminot, A., Kérouel, R., Hooker, B.A., Peterson, B.J., 1999. A simple and precise method for measuring ammonium in marine and freshwater ecosystems. Can. J. Fish. Aquat. Sci. 56, 1801–1808. https://doi.org/10.1139/f99-128.

Horrigan, S.G., McCarthy, J.J., 1982. Phytoplankton uptake of ammonium and urea during growth on oxidized forms of nitrogen. J. Plankton Res. 4, 379–389. https://doi.org/10.1093/plankt/4.2.379.

Ivančič, I., Degobbis, D., 1984. An optimal manual procedure for ammonia analysis in natural waters by the indophenol blue method. Water Res. 18, 1143–1147. https://doi.org/10.1016/0043-1354(84)90230-6.

Jauffrais, T., Drouet, S., Turpin, V., Méléder, V., Jesus, B., Cognie, B., Raimbault, P., Cosson, R.P., Decottignies, P., Martin-Jézéquel, V., 2015. Growth and biochemical composition of a microphytobenthic diatom (Entomoneis paludosa) exposed to shorebird (Calidris alpina) droppings. J. Exp. Mar. Biol. Ecol. 469, 83–92. https://doi.org/10.1016/j.jembe.2015.04.014.

Jézéquel, D., Brayner, R., Metzger, E., Viollier, E., Prévot, F., Fiévet, F., 2007. Two-dimensional determination of dissolved iron and sulfur species in marine sediment pore-waters by thin-film based imaging. Thau lagoon (France). Estuar. Coast. Shelf Sci. 72, 420–431. Biogeochemical and contaminant cycling in sediments from a human-impacted coastal lagoon. https://doi.org/10.1016/j.ecss.2006.11.031.

Kérouel, R., Aminot, A., 1997. Fluorometric determination of ammonia in sea and estuarine waters by direct segmented flow analysis. Mar. Chem. 57, 265–275. https://doi.org/10.1016/S0304-4203(97)00040-6.

Krom, M.D., 1980. Spectrophotometric determination of ammonia: a study of a modified Berthelot reaction using salicylate and dichloroisocyanurate. Analyst 105, 305–316. https://doi.org/10.1039/AN9800500305.

Luther, G.W., Sundby, B., Lewis, B.L., Brendel, P.J., Silverberg, N., 1997. Interactions of manganese with the nitrogen cycle: alternative pathways to dinitrogen. Geochim. Cosmochim. Acta 61, 4043–4052. https://doi.org/10.1016/S0016-7037(97)00239-1.

Méléder, V., Barillé, L., Rincé, Y., Morançais, M., Rosa, P., Gaudin, P., 2005. Spatio-temporal changes in microphytobenthos structure analysed by pigment composition in a macrotidal flat (Bourgneuf Bay, France). Mar. Ecol. Prog. Ser. 297, 83–99. https://doi.org/10.3354/meps297083.

Metzger, E., Simonucci, C., Viollier, E., Sarazin, G., Prévot, F., Jézéquel, D., 2007. Benthic response to shellfish farming in Thau lagoon: pore water signature. Estuar. Coast Shelf Sci. 72, 406–419. https://doi.org/10.1016/j.ecss.2006.11.011.

Metzger, E., Thibault de Chanvalon, A., Cesbron, F., Barbe, A., Launeau, P., Jézéquel, D., Mouret, A., 2016. Simultaneous nitrite/nitrate imagery at millimeter scale through the water–sediment interface. Environ. Sci. Technol. 50, 8818–8195. https://doi.org/10.1021/acs.est.6b00187.

Millero, F.J., Feistel, R., Wright, D.G., McDougall, T.J., 2008. The composition of standard seawater and the definition of the reference-composition salinity scale. Deep-Sea Res. Part A Oceanogr. Res. Pap. 55, 50–72. https://doi.org/10.1016/j.dsr.2007.10.001.

Mucci, A., Sundby, B., Gehlen, M., Arakaki, T., Zhong, S., Silverberg, N., 2000. The fate of carbon in continental shelf sediments of eastern Canada: a case study. Deep Sea Res. Part II Top. Stud. Oceanogr. 47, 733–760. https://doi.org/10.1016/S0967-0645(99)00124-1.

Mudroch, A., MacKnight, S.D., 1994. Handbook of Techniques for Aquatic Sediments Sampling. CRC Press.

Pagès, A., Teasdale, P.R., Robertson, D., Bennett, W.W., Schäfer, J., Welsh, D.T., 2011. Representative measurement of two-dimensional reactive phosphate distributions and co-distributed iron(II) and sulfide in seagrass sediment porewaters. Chemosphere 85, 1256–1261. https://doi.org/10.1016/j.chemosphere.2011.07.020.

Patton, C.J., Crouch, S.R., 1977. Spectrophotometric and kinetics investigation of the Berthelot reaction for the determination of ammonia. Anal. Chem. 49, 464–469. https://doi.org/10.1021/ac50011a034.

Regnault, M., 1987. Nitrogen excretion in marine and fresh-water Crustacea. Biol. Rev. 62, 1–24. https://doi.org/10.1111/j.1469-185X.1987.tb00623.x.

Riley, J.P., 1953. The spectrophotometric determination of ammonia in natural waters with particular reference to sea-water. Anal. Chim. Acta 9, 575–589. https://doi.org/10.1016/S0003-2670(01)80817-5.

Robertson, D., Teasdale, P.R., Welsh, D.T., 2008. A novel gel-based technique for the high resolution, two-dimensional determination of iron (II) and sulfide in sediment. Limnol Oceanogr. Methods 6, 502–512. https://doi.org/10.4319/lom.2008.6.502.

Roskam, K.T., De Langen, D., 1964. A simple colorimetric method for the determination of ammonia in seawater. Anal. Chim. Acta 30, 56–59. https://doi.org/10.1016/S0003-2670(00)88684-5.

Santos, I.R., Eyre, B.D., Huettel, M., 2012. The driving forces of porewater and groundwater flow in permeable coastal sediments: a review. Estuar. Coast Shelf Sci. 98, 1–15. https://doi.org/10.1016/j.ecss.2011.10.024.

Santner, J., Larsen, M., Kreuzeder, A., Glud, R.N., 2015. Two decades of chemical imaging of solutes in sediments and soils – a review. Anal. Chim. Acta 878, 9–42. https://doi.org/10.1016/j.aca.2015.02.006.

Sarazin, G., Michard, G., Prevot, F., 1999. A rapid and accurate spectroscopic method for alkalinity measurements in sea water samples. Water Res. 33, 290–294. https://doi.org/10.1016/S0043-1354(98)00168-7.

Schneider, C.A., Rasband, W.S., Eliceiri, K.W., 2012. NIH image to ImageJ: 25 years of image analysis [WWW document]. Nat. Methods. https://doi.org/10.1038/nmeth.2089.

Searle, P.L., 1984. The berthelot or indophenol reaction and its use in the analytical chemistry of nitrogen. A review. Analyst 109, 549–568. https://doi.org/10.1039/AN9840900549.

Strömberg, N., 2008. Determination of ammonium turnover and flow patterns close to roots using imaging optodes. Environ. Sci. Technol. 42, 1630–1637. https://doi.org/10.1021/es071400q.

Thibault de Chanvalon, A., Metzger, E., Mouret, A., Cesbron, F., Knoery, J., Rozuel, E., Launeau, P., Nardelli, M.P., Jorissen, F.J., Geslin, E., 2015. Two-dimensional distribution of living benthic foraminifera in anoxic sediment layers of an estuarine mudflat (Loire estuary, France). Biogeosciences 12, 6219–6234. https://doi.org/10.5194/bg-12-6219-2015.

Thibault de Chanvalon, A., Mouret, A., Knoery, J., Geslin, E., Péron, O., Metzger, E., 2016. Manganese, Iron and Phosphorus Cycling in an Estuarine Mudflat, Loire, France. J. Sea Res., Recent and Past Sedimentary, Biogeochemical and Benthic Ecosystem Evolution of the Loire Estuary (Western France), vol 118, pp. 92–102. https://doi.org/10.1016/j.seares.2016.10.004.

Thibault de Chanvalon, A., Metzger, E., Mouret, A., Knoery, J., Geslin, E., Meysman, F.J.R., 2017. Two dimensional mapping of iron release in marine sediments at submillimetre scale. Mar. Chem. 191, 34–49. https://doi.org/10.1016/j.marchem.2016.04.003.

Tréguer, P.J., Rocha, C.L.D.L., 2013. The world ocean silica cycle. Annu. Rev. Mar. Sci. 5, 477–501. https://doi.org/10.1146/annurev-marine-121211-172346.

Welker, C., Sdrigotti, E., Covelli, S., Faganeli, J., 2002. Microphytobenthos in the Gulf of Trieste (Northern adriatic sea): relationship with labile sedimentary organic matter and nutrients. Estuar. Coast Shelf Sci. 55, 259–273. https://doi.org/10.1006/ecss.2001.0901.

Welsh, D.T., Castadelli, G., 2004. Bacterial nitrification activity directly associated with isolated benthic marine animals. Mar. Biol. 144, 1029–1037. https://doi.org/10.1007/s00227-003-1252-z.

Yücel, M., 2013. Down the thermodynamic ladder: a comparative study of marine redox gradients across diverse sedimentary environments. Estuar. Coast Shelf Sci. 131, 83–92. https://doi.org/10.1016/j.ecss.2013.07.013.